



BIULETYN WAT  
ROK XLVI, NR 2, 2000

## Influence of protons on oxide compounds applied in optoelectronic devices

SŁAWOMIR MAKSYMILIAN KACZMAREK<sup>\*</sup>, JOLANTA WOJTKOWSKA<sup>\*\*</sup>,  
ZBIGNIEW MOROZ<sup>\*\*\*</sup>, JAROSŁAW KISIELEWSKI<sup>\*\*\*</sup>

<sup>\*</sup> Institute of Optoelectronics, M.U.T., 2 Kaliski Str., 000-908 Warsaw,

<sup>\*\*</sup> So<sup>3</sup>tan Institute of Nuclear Studies, 05-400 Œwierk

<sup>\*\*\*</sup> Institute of Electronic Materials Technology, 133 Wólczyńska Str., 01-919  
Warsaw

**Abstract.** Changes in optical properties of some oxide compounds (YAG, YAG: Nd<sup>3+</sup>, YAG: Ce<sup>3+</sup>, YAG: Ce<sup>3+</sup>, Mg<sup>2+</sup>, YAG: Cr<sup>3+</sup>, YAG: Cr<sup>4+</sup>, SrLaGa<sub>3</sub>O<sub>7</sub>: Dy<sup>3+</sup>, SrLaGa<sub>3</sub>O<sub>7</sub>: Cr<sup>3+</sup>, SrGdGa<sub>3</sub>O<sub>7</sub>: Cr<sup>3+</sup> and LiNbO<sub>3</sub>: Cu<sup>2+</sup>) induced by 21 MeV proton irradiation were studied. In the optical absorption spectra lines which belong to optically active dopants (like Ce<sup>3+</sup>, Cr<sup>3+</sup>, Fe<sup>3+</sup>) and F-type color centers are seen. Influence of proton irradiation on such centers is observed. It seems to be attributed to the ionization and/or recombination of definite centers. Moreover, for relatively high proton fluencies, Frenkel defects are probably created.

**Keywords:** additional absorption, proton irradiation, recombination, Frenkel defects

**Symbole UKD:**

### 1. Introduction

Changes of optical properties of various crystals induced by ionizing radiation are of big importance because many optical instruments is dedicated to work in radiation fields. For example, rockets launching the instrumentation to the space

are subjected to intensive proton exposure with the energy spectrum in the range from a few eV to about 100 MeV [1]. Except of pure military applications, optical instruments are installed on satellites and spacecraft missions, as well as in scientific laboratories, working on-line with accelerators. In general, the irradiation causes a degradation of optical properties of such instruments but, in some cases, irradiation may improve properties of optical materials so that, in principle, one can use irradiation as a kind of technological tool.

Among different kinds of radiation, studying of influence of irradiation by gamma photons and high energy electrons are the most frequently applied. Also an influence of neutrons from nuclear reactors is often studied. Quite recently irradiation by highly relativistic electrons, protons as well as heavy ions (with energies in GeV energy region) became popular.

Irradiation with low and medium energy protons, seems to be the less exploited, in spite of big importance of that kind of irradiation. Relative facility of getting large proton fluxes, in comparison e.g. with fast neutrons, makes such studies attractive. But, on the other hand, continuous energy change of protons along its trajectory in the medium causes some very serious computational ambiguities and difficulties.

In spite of quite large literature on the subject, understanding of physical phenomena induced by ionizing radiation in optically active crystals is still in its beginning stage. Some difficulties exists both, in experimental studies and in the theoretical calculations. This problem will be discussed below.

### **1.1. General features of interactions of particles with solids**

Main features of the interaction of the ionizing particles with solids can be summarized as follows:

(i) charged particles, contrary to neutral ones, passing through the matter lose continuously their energy mainly due to the ionization of the medium atoms;

(ii) interaction of particles can be treated as interaction with two atomic separate subsystems: electronic and nuclear one. To a good approximation these two interactions are decoupled;

(iii) fast incident particles initialize a stochastic cascade. There is essential difference between cascades initiated by photon or electron (electromagnetic cascade caused by electromagnetic interactions) and protons or other heavy particles (hadronic cascade, caused by electromagnetic and nuclear interactions). Both kinds of cascades can be described only in a probabilistic way;

(iv) after the fast cascade is finished, much slower interactions with the medium still take place.

Defects in crystals can be produced by ionizing radiation as well as destroyed or modified. The last effects concern also defects which were initially present in

the sample, before its irradiation. One can list many kinds of produced defects such as: (i) ionized atoms constituting original lattice in the interstitial positions, (ii) vacancies, (iii) intruder atoms or ions (knocked-out atoms of the lattice, stopped products of nuclear reactions etc.). The original defects can be further modified by recombination or by evolution driven by the interaction with the lattice.

## 1.2. Some particular mechanisms and theories

The interaction of medium energy protons in crystals cannot be considered separately out of the interaction of heavy multicharged ions. It is so because the fast heavy ions are always recoiled in elastic nuclear scattering of protons and constitute nuclear reaction products which influence the production of crystal defects.

The most important steps of charged particle interaction are:

(i) Electronic and nuclear energy loss along the particle trajectory in medium. Here, standard versions of theory obey [2-6];

(ii) Development of the cascade, emission of primary knocked-out atoms (PKA's) and initial damage distributions in the crystal. Here, two main approaches are: conventional Monte Carlo (MC) for amorphous media [7] and binary collision (BC) codes including crystal structure [8]. In the last stage of the cascade development, more complex molecular dynamics (MD) codes are used including in a natural way the many-body interaction between atoms of the crystal lattice [9];

(iii) Redistribution of initial electronic excitations and their relaxation. Here, initial electron spectra (delta electrons) are calculated including different mechanisms of their production (three-body-encounter (TBA), Auger electrons, electron-loss-to the continuum (ELC), target electron capture to the continuum (ECC) and binary encounter electrons (BE)) [10]. Relaxation of initial distribution of electronic excitations include such mechanisms as: cooling-down up to thermal equilibrium with lattice (electron-phonon interaction) [11], radiative deexcitation (X, UV-, visible photon emission [12], Auger electron emission [13]), radiationless breaking the electronic bonds of the lattice (including production of defects) [14];

(iv) Evolution and modification of primary defects in the crystal lattice. This is due to the recombination of primary defects by excited electrons, annealing of defects by the thermal spike, interaction of primary defects with defect sinks and defect agglomeration [15]. It is worthwhile to realize, that only due to the interaction of primary PD's with the delta electron cloud from the same cascade a very small part of the original population (of the order of 1%) survive [16] and they are further modified by the interaction with the lattice.

Thus, interaction of charged particle with the crystal medium appears to be very complex. Especially, if one want to watch the evolution of the process leading to the production of color or optically active Frenkel centers. Properties of these optically active defects to a high degree are determined by the interaction with

surrounding atoms of the crystal lattice. Much more, than e.g. defects deciding about the electrical properties of the semiconductors. Therefore in the last stages of the excitation relaxation the use of very complicated MD methods is unavoidable. Effective use of these methods is, in fact, in its initial stage. Moreover, except of complex mathematical procedures it require using reach data base describing detailed properties of the interaction of particles and crystal lattice. Thus, at present, it is rather hard to predict or explain theoretically changes of optical properties of crystals under irradiation, as yet and collection of more experimental data is very desirable. This concerns also particular oxide crystals being the subject of the present work.

In the next sections of this work we report the most important effects recently found by us during our study of the influence of the irradiation by 21 MeV protons on the optical absorption spectra of various crystals containing oxide compounds. At the end we discuss some of them in terms of the theory of the proton-crystal interaction.

## 2. Experimental

From the single crystals obtained in Institute of Electronic Materials Technology the parallel plate samples of 1-3 mm thick were cut-out and both sides polished: YAG: Ce (0.1 at. % Ce), Ce: YAG: Ce (0.2 at. % Ce), YAG: Ce, Mg (0.2 at. % Ce + 0.1 at. % Mg), YAG: Cr<sup>4+</sup> (0.1 at. % Cr), YAG: Cr<sup>3+</sup>, obtained by annealing of YAG: Cr<sup>4+</sup> single crystal in reducing atmosphere at 1200°C for 1h, SrLaGa<sub>3</sub>O<sub>7</sub>: Dy<sup>3+</sup> (1 at. % Dy), SrLaGa<sub>3</sub>O<sub>7</sub>: Cr (0.1 at. % Cr) and LiNbO<sub>3</sub>: Cu (0.06 at. % Cu). Proton exposures were done in the C30 cyclotron in INP Łwówek. The proton fluency was varied between 5\*10<sup>12</sup> to about 1.2\*10<sup>16</sup> protons/cm<sup>2</sup>. Each time the fluency was measured with a charge integrator. To avoid the sample overheating the average beam current was kept at approximately 200 nA. Collimated to about 10 mm in diameter external proton beam passed through the few cm long air gap, where the crystal samples were placed. Effective proton energy at the entrance face of the sample was ca. 21 MeV.

The absorption spectra were taken at 300 K before and after proton irradiation in the spectral range between 190 - 25 000 nm using LAMBDA-2 PERKIN-ELMER, ACTA VII BECKMAN and FTIR 1725 PERKIN-ELMER spectrophotometers. Values of  $\Delta K(\lambda)$  factors which describe an additional absorption due to the irradiation were calculated according to the formula:

$$DK(I) = \frac{1}{d} \ln \frac{T_1}{T_2}, \quad (1)$$

where  $K$  is absorption,  $DK(I)$  is the additional absorption,  $I$  is the wavelength,  $d$  is the sample thickness, and  $T_1$  and  $T_2$  are the transmissions of the sample measured before and after irradiation, respectively.

All the samples were irradiated for "as grown" as well as after annealing of as grown crystals at 1400°C for 3h in the oxidizing atmosphere (YAG's) and at 1200°C for 1h in reducing atmosphere.

### 3. Results and discussion

Presented in Fig. 1 absorption spectrum of YAG: Ce (0.1 at. % Ce) single crystal shows two peaks at about 340 nm and 460 nm, which are attributed to  $Ce^{3+}$  dopant ions. It is shown that annealing at 1400°C prior to irradiation (curve 1), causes local decrease in absorption in the vicinity of the above mentioned peaks. After bombarding with  $10^{14}$  protons/cm<sup>2</sup> a strong rise in absorption is observed (curve 2). Such behavior of absorption spectrum is caused probably by the change in  $Ce^{3+}$  concentration.

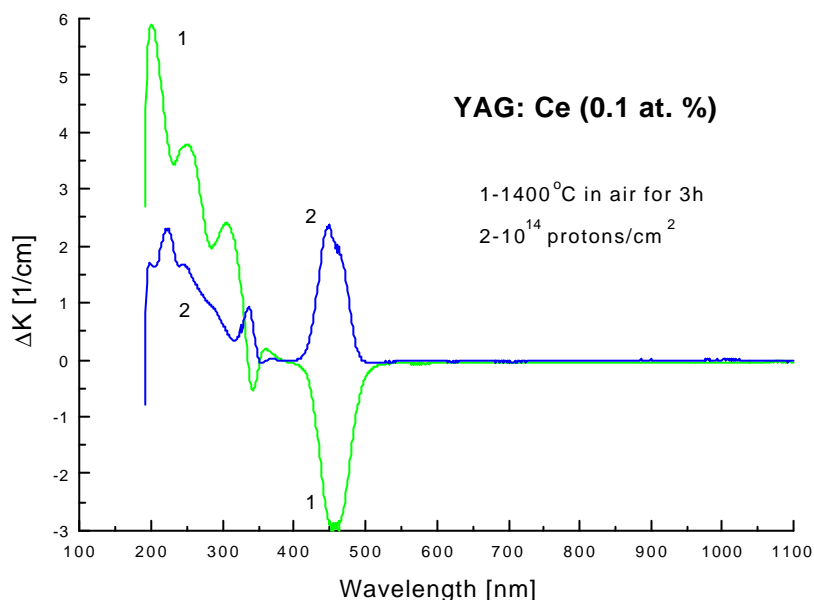


Fig. 1. Additional absorption in: YAG: Ce (0.1 at. %) single crystal after: (1) – annealing in air at 1400°C for 3h and, (2) – proton irradiation with a fluency of  $10^{14}$  protons/cm<sup>2</sup>

Similar changes in absorption spectrum are observed also for YAG: Ce, Mg (0.2 at. %, 0.1 at. %) single crystal after its annealing in air at 1400°C for 3h and

irradiation with protons with a fluency of  $10^{14}$  protons/cm<sup>2</sup>, as shown in Fig. 2 (curves 1 and 2). This rise continues for  $2 \cdot 10^{14}$  protons/cm<sup>2</sup> (curve 3), where it reaches its maximum. At  $3 \cdot 10^{14}$  protons/cm<sup>2</sup> a significant drop of absorption is observed (curve 4). Dose dependence of additional absorption after proton irradiation of 475 nm Ce<sup>3+</sup> peak for the crystal is seen in the insert of Fig. 2. One can see distinct maximum of this curve at about  $2 \cdot 10^{14}$  protons/cm<sup>2</sup>.

In our opinion, for a fluency of  $10^{14}$  protons/cm<sup>2</sup> mainly recombination process of the type Ce<sup>4+</sup> → Ce<sup>3+</sup> occur (an increase in Ce<sup>3+</sup> concentration), while in the range of  $2 \cdot 10^{14}$  -  $3 \cdot 10^{14}$  protons/cm<sup>2</sup> also ionization Ce<sup>3+</sup> → Ce<sup>4+</sup> is observed (a decrease in Ce<sup>3+</sup> concentration with respect to previous irradiation). An increase in the Ce<sup>3+</sup> concentration after irradiation of all the studied samples with proton beams (Figs. 1 and 2), consistently suggest the presence of the Ce<sup>4+</sup> ions in all of our samples just before irradiation. Distortion of the heavily concentrated sample, seen in Fig. 2 for a wavelength about 458 nm, may be due to inhomogeneous effect takes place. The double structure of additional absorption band looks like anti-correlation. With pretty thick sample (1 mm) and high Ce<sup>3+</sup> absorption coefficient (and high content of Ce<sup>3+</sup>), the light transmission near the max. at 458 nm may be extremely poor. In such situation, it can compete with the efficient fluorescence of Ce<sup>3+</sup>.

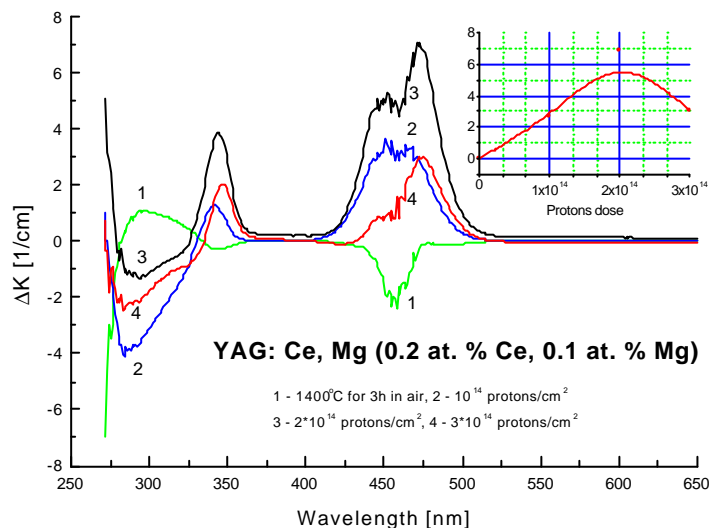


Fig. 2. Additional absorption in Ce, Mg: YAG (0.2 at. %, 0.1 at. %) single crystal after (1) annealing in air at 1400°C for 3h and subsequent irradiation with protons with fluencies: (2) –  $10^{14}$ , (3) –  $2 \cdot 10^{14}$  and (4) –  $3 \cdot 10^{14}$  protons/cm<sup>2</sup>. Insert: dose dependence of 475 nm Ce<sup>3+</sup> peak

In Fig. 2 one can also observe changes in  $\text{Mg}^{2+}$  ion absorption spectrum seen in the vicinity of 275 nm which indicate change in Mg valency (mainly ionization  $\text{Mg}^{2+} \rightarrow \text{Mg}^{3+}$ ) after proton irradiation.

In Fig. 3 absorption ( $K$ ) and changes in absorption ( $\Delta K$ ) of  $\text{YAG:Cr}^{3+}$  single crystal, obtained by annealing of  $\text{YAG:Cr}^{4+}$  single crystal in reducing atmosphere for 1h, after subsequent proton irradiations are presented. As seen the absorption curve of  $\text{YAG:Cr}^{3+}$  single crystal (curve 1) show two peaks at about 430 and 600 nm characteristic for  $\text{Cr}^{3+}$  transitions. Small fluencies of protons lead to an increase (curves 2-4) in  $\text{Cr}^{3+}$  ion concentration (an increase in absorption of  $\text{YAG:Cr}^{3+}$  single crystal in the range of  $\text{Cr}^{3+}$  transitions) while fluency of  $10^{14}$  protons/cm<sup>2</sup> leads to an increase in  $\text{Cr}^{4+}$  ion concentration (curve 5 with a maximum at about 480 nm). Thus, similarly as for  $\text{YAG:Ce}$  single crystal, we observe change in a mechanism of protons interaction with  $\text{YAG:Cr}^{3+}$  crystal with protons fluency, from recombination process of the type  $\text{Cr}^{4+} \rightarrow \text{Cr}^{3+}$  to ionization  $\text{Cr}^{3+} \rightarrow \text{Cr}^{4+}$ . May be not all  $\text{Cr}^{4+}$  ions were reduced to  $\text{Cr}^{3+}$  after annealing process of  $\text{YAG:Cr}^{4+}$  single crystal in reducing atmosphere.

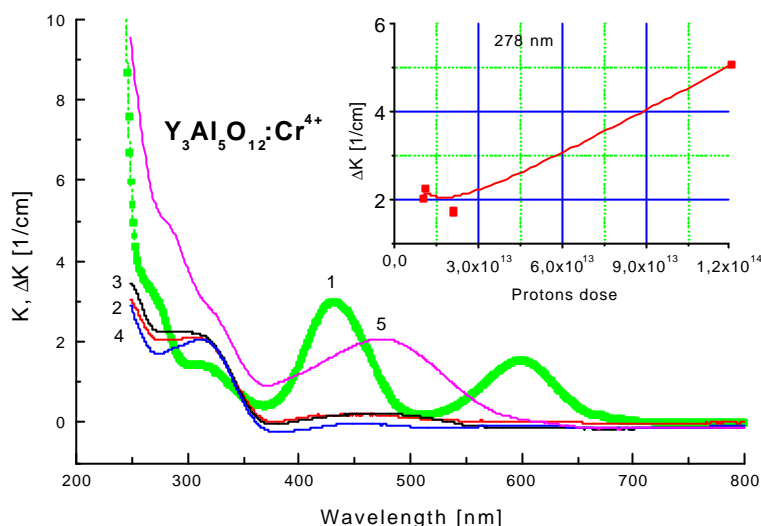


Fig. 3. Absorption (curve 1) and changes in absorption (curves 2-5) of  $\text{YAG:Cr}^{3+}$  single crystal after subsequent fluencies: (2) –  $1 \cdot 10^{12}$ , (3) –  $1.1 \cdot 10^{13}$ , (4) –  $2.1 \cdot 10^{13}$  and, (5) –  $1.21 \cdot 10^{14}$  protons/cm<sup>2</sup>.  
Insert: dose dependence of 278 nm peak

In the insert of Fig. 3 dose dependence of additional absorption after proton irradiation is seen, where minimum associated with a change of the mechanism of interaction of protons with  $\text{YAG:Cr}^{3+}$  single crystal is observed.

In Fig. 4 changes in absorption of YAG (Fig. 4b) and YAG: Nd (1 at. %) (Fig. 4a) single crystals are presented after proton irradiations for fluencies from  $10^{13}$  to  $10^{16}$  protons/cm<sup>2</sup>. There are seen characteristic for YAG matrix radiation defects, e.g. 276 nm and 300 nm (Fe<sup>2+</sup> and Fe<sup>3+</sup> ions) and 450 nm (F centers). For doses lower than  $10^{14}$  protons/cm<sup>2</sup> (curves 1-3 in Fig. 4a and curves 1 and 2 in Fig. 4b) we observe recharging processes of Fe ions and F centers, while for fluencies greater than  $10^{14}$  protons/cm<sup>2</sup> (curves 4 and 6 in Fig. 4a and curves 3 and 4 in Fig. 4b) ionizing is observed also. The strong increase in additional absorption over  $10^{15}$  protons/cm<sup>2</sup> may be due to Frenkel defects.

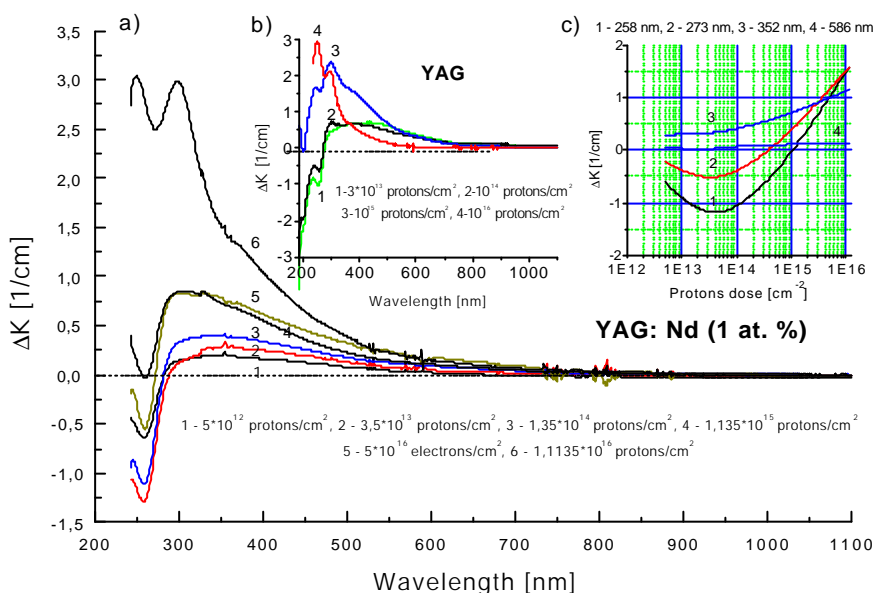


Fig. 4. Additional absorption of YAG (a) and YAG: Nd (b) single crystals after protons irradiation with fluencies from  $5 \cdot 10^{12}$  to  $1.1135 \cdot 10^{16}$  protons/cm<sup>2</sup>. For comparison additional absorption after electrons irradiation is presented with a fluency of  $5 \cdot 10^{16}$  electrons/cm<sup>2</sup> (curve 5 in Fig. 4a). Fig. 4c presents dose dependence of additional absorption after protons irradiation of YAG: Nd single crystal for wavelengths: 258, 273, 352 and 586 nm

In Fig. 4c dose dependence is presented of additional absorption of YAG: Nd single crystal for wavelengths: 258, 273, 352 and 586 nm. For all the wavelengths a minimum is seen for a dose of about  $10^{14}$  protons/cm<sup>2</sup>, moreover, as seen, a rise in absorption is greater for shorter wavelengths.

Curve 5 in Fig. 4a shows additional absorption band of YAG: Nd single crystal after electrons irradiation with a fluency of  $5 \cdot 10^{16}$  electrons/cm<sup>2</sup>. Comparing curves 4 and 5 one can see that the difference between the two irradiations is the



type of recharging process of Fe ions mainly. It seems that for protons ionization fraction is greater than for electrons (shallower minimum of additional absorption for about 258 nm). Generally different color centers are observed and different relative intensities of those peaks which belong to the same kind of defects are observed for samples bombarded with gamma's, electrons and protons.

From the above four figures the following general features of the changes in absorption spectra after proton irradiation can be extracted: (i) local extremes in the range of active ions transitions suggesting their valency change, (ii) flat absorption extreme at about  $10^{14}$  protons/cm<sup>2</sup>; (iii) Shallow minimum at about  $10^{15}$  protons/cm<sup>2</sup>; (iv) further monotonic rise at fluencies in the range between  $10^{15}$  and  $10^{16}$  protons/cm<sup>2</sup>; (iv) substantial differences exhibit curves measured for different wavelengths and different ionizing particles.

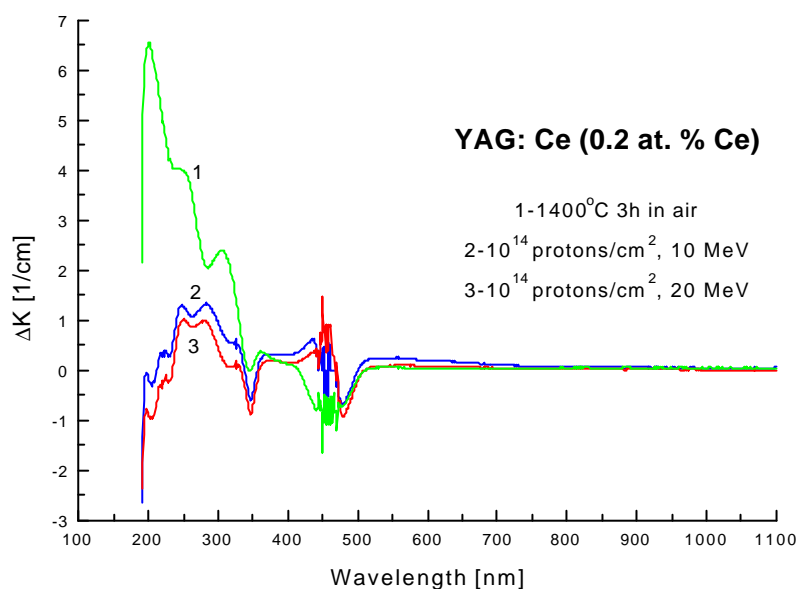


Fig. 5. Additional absorption in YAG: Ce (0.2 at. %) single crystal after (1) annealing in air at 1400°C for 3h and protons irradiation with a dose of  $10^{14}$  protons/cm<sup>2</sup> and with an energy: (2) – 10 MeV and (3) – 20 MeV

Simultaneous bombarding with protons of two parts of the same sample with different initial energies (20 and 10 MeV, obtained by using the energy degrading foil at the entrance of the sample) have indicated some differences in the absorption spectra. These differences appear to be not very strong (see Fig. 5) and have quantitative rather than qualitative character. From this we conclude, that decisive role for optical properties of crystals has the low energy end of proton trajectory.

In Fig 6, where additional absorption spectra of  $\text{SrLaGa}_3\text{O}_7:\text{Dy}$  (1 at. %) single crystal are shown after proton irradiation with fluencies up to  $10^{16}$  protons/ $\text{cm}^2$ , a radiation induced shift of the short-wavelength absorption edge is seen. Moreover, for this sample additional absorption appears to be much stronger than for the described above YAG crystals.

The reason of such effect is interpreted by us as radiation induced electron exchange  $\text{Ga}^{3+} \rightarrow \text{Ga}^{2+}$ . This was confirmed by additional ESR measurements [17]. The obtained results can be explained by means of the following process:  $\text{Ga}^{3+}$  ion captures the electron which was knocked out from  $\text{O}^{2-}$  ion by proton irradiation and in a consequence,  $\text{Ga}^{2+}$  paramagnetic center is formed with a spin value equal to  $S = 1/2$ . The process can be illustrated by the following reactions:  $\text{O}^{2-} + \text{p}^+ \rightarrow \text{O}^{1-} + \text{e}^-$ ;  $\text{Ga}^{3+} + \text{e}^- \rightarrow \text{Ga}^{2+}$ .

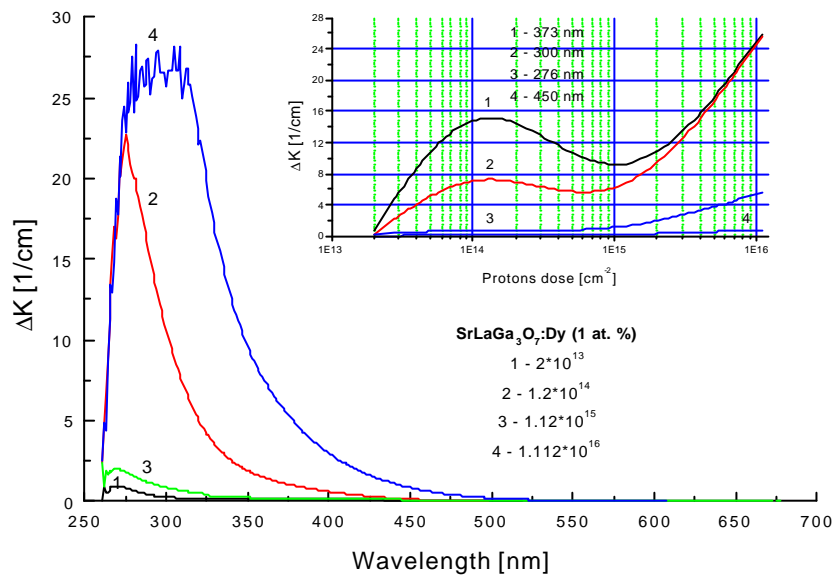


Fig. 6. Additional absorption bands in  $\text{SrLaGa}_3\text{O}_7:\text{Dy}$  (1 at. %) single crystal after proton irradiation with fluencies from  $2 \cdot 10^{12}$  to  $1.112 \cdot 10^{16}$  protons/ $\text{cm}^2$ . In the insert dose dependence of additional absorption is seen for wavelengths: 373, 300, 276 and 450 nm

The same phenomenon was observed for  $\text{SrLaGa}_3\text{O}_7:\text{Cr}$  and  $\text{SrGdGa}_3\text{O}_7:\text{Cr}$  single crystals [18], moreover, for these crystals changes in valency of  $\text{Cr}^{3+}$  ions were observed. The mechanism of these changes (recombination or ionization) was dependent on protons dose.

Thus, proton irradiation can also change the valency state of matrix ion (not only dopants).

In the insert of Fig. 6 dose dependence of additional absorption in SrLaGa<sub>3</sub>O<sub>7</sub>:Dy single crystals is seen, whose all the features confirm results described previously for YAG crystals (maximum at about 10<sup>14</sup> and minimum at about 10<sup>15</sup> protons/cm<sup>2</sup>).

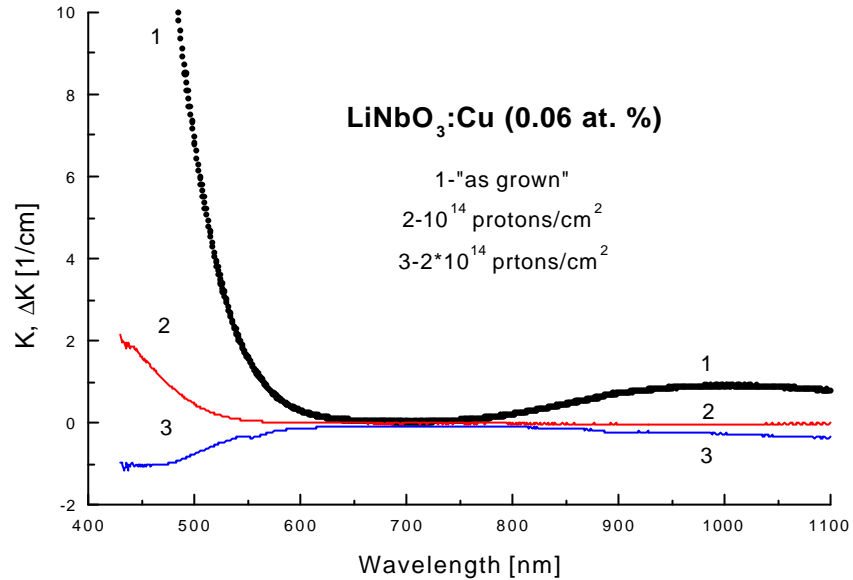


Fig. 7. Absorption (1) and additional absorption after proton irradiation with a fluency: 10<sup>14</sup> (2) and 2\*10<sup>14</sup> (3) protons/cm<sup>2</sup> in LiNbO<sub>3</sub>:Cu (0.06 at. %) single crystal

In Fig 7 an example of LiNbO<sub>3</sub>:Cu spectrum is shown, where it is clearly seen that in some region of the proton fluencies, the resulting crystal transparency can be higher (i.e.  $K$  is negative), than that of the same sample before the irradiation. Similar phenomenon was observed for Li<sub>2</sub>B<sub>4</sub>O<sub>7</sub> single crystals. Such behavior takes place probably due to annealing of irradiated crystals.

#### 4. Discussion

The characteristic rise and decrease of the absorption for Ce<sup>3+</sup> peaks at about 340nm and 460 nm ( Figs 1 and 2) is interpreted as a result of competition between recombination of Ce<sup>4+</sup> → Ce<sup>3+</sup> of fourvalent ions and ionization process Ce<sup>3+</sup> → Ce<sup>4+</sup>. As a result of 1400° C annealing prior to irradiation, a majority of Ce<sup>3+</sup> ions, originally left in the sample during crystallization, was recharged to Ce<sup>4+</sup>. Therefore radiation effects starts from their recombination, thus increasing the con-

centration of  $Ce^{3+}$  ions in the sample. But, in the course of irradiation, the competing ionization of  $Ce^{3+}$  begins to play more and more significant role. The same phenomenon takes place for  $Cr^{3+}$  and  $Cr^{4+}$  ions in YAG,  $SrLaGa_3O_7$  and  $SrGdGa_3O_7$  single crystals.

The whole process of the evolution of  $Ce^{3+}$  concentration can be mathematically described by the system of coupled differential master equations, of the kind:

$$d c_i / dt = \sum_k \{ P_{ki} * c_k - R_{ik} * c_i \} \quad ; \quad i=1,2,3,\dots \quad (2)$$

where  $c_i$  are concentrations of  $Ce^{4+}$ ,  $Ce^{3+}$  and  $Ce^{2+}$ , respectively and  $P_{ki}$  are build-up probabilities of  $c_i$  due to the recharging process  $k \rightarrow i$  and  $R_{ik}$  are probabilities of destruction of  $c_i$  due to the process  $i \rightarrow k$ . Coefficients  $P$  and  $R$  should, if necessary, include also concentration changes due to thermal annealing or other irradiation independent processes. Essentially, if the proton fluency is low enough, these coefficients should be linear with intensity of incident protons. However, for large fluencies, when an interaction between different proton trajectories is taken into account, they can have nonlinear terms as well. Such interaction causing nonlinear build-up of the dopant concentrations was recently observed in heavy ion irradiation of solid samples [19], where produced dopants were nonlinearly quenched by the mutual interaction of defects belonging to different particle trajectories if they became very close to each other. This effect became visible, when the total fluency of incident ions is large enough. In [19] the effective radius  $r_0$  of the moving ion trajectory cylinder was fitted and found to be about 20 nm. It seems to be very suggesting, that for incident protons, the position of the absorption maximum observed by us is at fluency of about  $2 \cdot 10^{14}$  particles/cm<sup>2</sup>, what corresponds to average radius of the circular area free of trajectories to be also about 20 nm.

Solution of the written above master equations require prior calculations of coefficients  $P_{ki}$  and  $R_{ik}$ , i.e. require knowledge of the corresponding cross sections for various recharging processes, which are dependent on particular crystal medium. At present it seems to be very complex and ambiguous procedure, which clearly exceeds frames of the present work.

Absorption dependence on the proton fluency of other wavelengths, belonging to the continuum spectrum, exhibit also characteristic maximum at about  $10^{14}$  protons/cm<sup>2</sup>. Moreover, for larger proton doses, after some minimum is reached, new fast monotonic rise of the absorption is observed at  $10^{15}$  and  $10^{16}$  protons/cm<sup>2</sup>. This last rise is interpreted as production of Frenkel defects, which are essentially vacancies or interstitial in the crystal lattice, and thus their production should be linear with the total proton fluency.

To compare effects of different radiations, one should recalculate, at first, doses and fluencies to some common system of units. To do this one can take into

account that the absorption of  $10^{14}$  protons/cm<sup>2</sup> of 20 MeV energy in the YAG crystal layer of 2 mm thickness corresponds to the absorbed dose of about 400 kGy. For 1 MeV electrons bombarding a sample of the same thickness, the corresponding dose is about 20 kGy.

Looking on Fig. 4 it is seen that the structure of the observed absorption spectrum depends not only on the absorbed dose, but also on the kind of ionizing particles. This is especially evident for protons, for which some peaks are seen which are not present for electrons and gammas. Also, for the same absorbed dose but different bombarding particles the general shape of spectra is quite different. It is especially evident in the region between 200 and 350 nm.

Decisive role of the low-energy end of the proton trajectory in the establishing the optical properties of crystal can be easily understood, taking into account that electronic energy loss  $S_e$ , which is responsible for ionization and inelastic excitation of the atomic electrons, strongly increase for lower proton energies. Therefore recharging processes should be stronger if initiated by a particle of lower energy. On the other hand, nuclear energy loss  $S_n$  leading to the production of defects due to nuclear scattering and nuclear reactions has valuable contribution to the total energy loss only at the end of the proton range [5, 20].

Concerning the short wavelength edge shift and improvement of the crystal transparency it is clearly is caused by radiation induced modification of the defects responsible for the optical properties of the crystal. Our present knowledge of the nature of the centers responsible for such effects in the crystals being the subject of our study is still not satisfactory, as yet, and it require further, more detailed both experimental as well as theoretical studies.

## 5. Conclusions

From the present studies of the absorption spectra modified by ca. 21 MeV proton irradiation we conclude that:

1. Irradiation by medium energy protons modifies absorption spectra and the following competing processes were recognized:

(i) electronic subsystem:

- ionization of three-valent dopant ions (i.e.  $Ce^{3+}$ ,  $Cr^{3+}$ ,  $Fe^{3+}$ );
- recombination of fourvalent ions ( $Ce^{4+}$ ,  $Cr^{4+}$ );
- simultaneous recharging process ( $Ga^{3+} O^{2-}$ )  $\rightarrow$  ( $Ga^{2+} O^{1-}$ )

(ii) nuclear subsystem:

- production of Frenkel defects, visible for proton fluencies over  $10^{15}$  protons/cm<sup>2</sup>

2. Fluency dependence of the absorption coefficients exhibit characteristic shape with maximum at about  $10^{14}$  protons/cm<sup>2</sup>, minimum at about  $10^{15}$  protons/cm<sup>2</sup> and further sharp rise for higher fluencies. Such non-monotonic depend-

ence is characteristic for color centers, rather than for Frenkel centers. For the later ones, a monotonic, linear with proton fluency dependence is seen. The probable reason of the decrease in the region  $2 \cdot 10^{14}$  -  $10^{15}$  protons/cm<sup>2</sup> could be competition between at least two different recharging processes, which may have nonlinear dependence of the coefficients in master equations of the proton intensity. One possible reason is mutual interaction of the cascades from different proton trajectories.

3. Decisive role in the modification of the optical properties of the studied samples has low-energy part of proton trajectory, i.e. the end of its range.

4. Further attempts require studies the origin of various fragments of the absorption spectra and, in particular, attempts to isolate contributions from the well defined lattice defects, other than listed above color centers. This would require extending the variety of the experimental techniques applied.

5. Calculations, from the first principles, of the production probabilities of different final color centers or optically active Frenkel defects in oxide compound crystals, being the subject of the present study, are still on its beginning stage. Before becoming to be really reliable, they require not only complex and tedious calculations but also an large increase of the existing data base, needed to calculate the coefficients and functions of master and molecular dynamic equations.

## 6. References

- 1 G. P. Summers et al., IEEE Trans. Nucl. Sci. 40 (93) 1372
- 2 H.A. Bethe, Ann. Phys. (Leipzig) 5 (1930) 325
- 3 F. Bloch, Ann. Phys. 16 (1933) 285
- 4 J. Linhardt, M. Sharff, H.E. Shiott, Mat. Fys. Medd. Danske Vid. Selsk. 33(14) (1963) 26
- 5 Y. Yavlinskii, NIM in Phys. Research, B155 (96) 594; W.H. Barkas, in Nulc. Res. Emulsions, (Academic Press, NY 1963, Vol 1, 371
- 6 J. Linhardt, A. Winther, Mat. Fys. Medd. Danske Vid. Selsk. 43(4?) 1964; J. Linhardt, Mat.Fys. Medd. Danske Vid. Selsk. 34(14) 1965; T. Ito et al., NIM in Phys.Research B135 (98) 132
- 7 W. Eckstein, "Computer Simulation of Ion-Solid Interaction", Springer, Berlin 1991; J. Ziegler, J.P. Biersack, U. Littmark, " The program package TRIM-91"; J. Ziegler, J.P. Biersack, U. Littmark, " The Stopping Power of Ions in Solids", Vol 1, Pergamon Press, NY'1985; M. Posselt, Radiat. Eff. 130/131 (94) 87; J.P. Biersack, W. Eckstein, Appl.Phys. 34(84) 73
- 8 O.S. Oen, M.T. Robinson, NIM 12 (76) 647; M.T. Robinson, Phys.Rev., B40 (89) 10717; M. Hou, NIM 132 (76) 641
- 9 K. Nortlund, A. Kuronen, NIM in Phys. Research B115 (1996) 528
- 10 U. Bechthold et al., NIM in Phys.Research B143, No4 (98) 441
- 11 Y. Yavlinskii, NIM in Phys.Research, B155 (96) 594
- 12 V.J. Kennedy et al., NIM in Phys. Research, B134 (98) 165
- 13 N. Stolterfocht, Phys.Rep. 146 (87), 315
- 14 N. Itoh, NIM in Phys.Research, B135 (98) 175
- 15 Z. Wang NIM B146 (98) 290
- 16 Z. Wang NIM in Phys. Research B 135(98) 265

- 17 S. M. Kaczmarek, R. Jabłoński, I. Pracka, G. Boulon, T. Łukasiewicz, Z. Moroz and S. Warchoń, „Radiation Defects in SrLaGa<sub>3</sub>O<sub>7</sub> Crystals Doped With Rare-Earth Elements”, *Nuclear Instruments and Methods Section B, Beam Interactions with Materials and Atoms*, B142, 1998, 515-522
- 18 S.M. Kaczmarek, M. Berkowski, R. Jabłoński, „Recharging processes of chromium ions in SrGdGa<sub>3</sub>O<sub>7</sub> single crystals”, *Crystal Research and Technology*, vol. 34 (8), 1999
- 19 C. Trautmann et.al. NIM B146 (98) 967
- [20] J. Linhardt, Proc. Roy. Soc. A311,(69),11

## Oddziaływanie protonów z materiałami tlenkowymi stosowanymi w urządzeniach optoelektronicznych

**Streszczenie.** Badano zmiany właściwości optycznych materiałów tlenkowych (YAG, YAG: Nd<sup>3+</sup>, YAG: Ce<sup>3+</sup>, YAG: Ce<sup>3+</sup>, Mg<sup>2+</sup>, YAG: Cr<sup>3+</sup>, YAG: Cr<sup>4+</sup>, SrLaGa<sub>3</sub>O<sub>7</sub>: Dy<sup>3+</sup>, SrLaGa<sub>3</sub>O<sub>7</sub>: Cr<sup>3+</sup>, SrGdGa<sub>3</sub>O<sub>7</sub>:Cr<sup>3+</sup> oraz LiNbO<sub>3</sub>: Cu<sup>2+</sup>) indukowane przez wiązkę protonów o energii 21 MeV z cyklotronu. Wśród linii absorpcyjnych obserwowano linie należące do domieszek aktywnych (jak Ce<sup>3+</sup>, Cr<sup>3+</sup>, Fe<sup>3+</sup>) oraz do centrów barwnych typu F. Oddziaływanie protonów na te centra wydaje się być związane z jonizacją i/lub rekombinacją powyższych centrów. Ponadto, dla względnie wysokich strumieni protonów (10<sup>14</sup> protonów/cm<sup>2</sup>), obserwuje się powstawanie defektów Frenkla.